[9]H. J. Fossum and A. Rannestad, J. Appl. Phys. 38, 5177 (1967).
[10]K. K. Thornber and R. P. Feynman, Phys. Rev. B 1, 4099 (1970).
[11]R. C. Hughes, Appl. Phys. Lett. 21, 196 (1972).
[12]D. J. Howarth and E. H. Sondheimer, Proc. Roy. Soc., Ser. A 219, 53 (1953).
[13]R. P. Feynman, R. W. Hellwarth, C. K. Iddings, and P. M. Platzman, Phys. Rev. 127, 1004 (1962).
[14]H. Fröhlich, Advan. Phys. 3, 325 (1954).
[15]F. S. Goulding and Y. Stone, Science 170, 280 (1970).
[16]L. B. Loeb, in *Handbuch der Physik*, edited by S. Flügge (Springer, Berlin, 1956), Vol. XXI, p. 471.
[17]A. Hummel and A. O. Allen, J. Chem. Phys. 46, 1602 (1967).
[18]R. C. Hughes, IEEE Trans. Nucl. Sci. 18, 281 (1971).
[19]M. Lax, Phys. Rev. 119, 1502 (1960).
[20]L. Onsager, Phys. Rev. 54, 554 (1938).
[21]J. H. Konneat, J. Karle, and G. A. Ferguson, Science 179, 177 (1973).
[22]L. Friedman, J. Non-Cryst. Solids 6, 329 (1971).
[23]D. Emin, C. H. Seager, and R. K. Quinn, Phys. Rev. Lett. 28, 813 (1972).
[24]N. F. Mott, Phil. Mag. 22, 7 (1970).

Observation of the Decay $K_L^0 \to \mu^+\mu^-$†

W. C. Carithers,* T. Modis, D. R. Nygren, T. P. Pun, E. L. Schwartz, and H. Sticker
Columbia University, New York, New York 10533

and

J. Steinberger and P. Weilhammer
CERN, Geneva, Switzerland

and

J. H. Christenson
New York University, New York, New York 10012

(Received 16 April 1973)

An experiment performed at the Brookhaven National Laboratory alternating-gradient synchrotron has yielded six events above negligible background which satisfy criteria for the decay $K_L^0 \to \mu^+\mu^-$. The K_L^0 flux, measured by means of the decay $K_L^0 \to \pi^+\pi^-$, leads to a value for the branching ratio $\Gamma(K_L^0 \to \mu^+\mu^-)/\Gamma(K_L \to \text{all}) = 11 \times 10^{-9}$.

The decay $K_L^0 \to \mu^+\mu^-$ is expected to occur with a branching ratio of at least 6×10^{-9}.[1] This prediction is based on unitarity, the measured $K_L^0 \to \gamma\gamma$ rate, quantum electrodynamics, and the assumption that contributions from intermediate states other than $K_L^0 \to \gamma\gamma$ are negligible. Theoretical estimates of the maximum interference possible from other likely intermediate states do not reduce this lower bound substantially.[2] The experiment of Clark *et al.*,[3] however, places an upper limit of 1.8×10^{-9} (90% confidence level) on this decay, a value incompatible with this prediction and difficult to resolve theoretically without introduction of new particles or interaction mechanisms. The present work was undertaken as a check of the experimental result of Clark *et al.*

The apparatus was situated in a long-lived neutral beam derived from the G-10 internal target of the Brookhaven National Laboratory alternating-gradient synchrotron. Three collimators defined a solid angle of 18 μsr at an angle of 4.7° to the circulating proton beam. 8 radiation lengths of lead near the first collimator converted γ rays and two sweeping magnets eliminated charged particles from the beam. The final 13 m of the beam line, as well as the 6-m decay region, were evacuated.

K_L^0 decays were detected with a spectrometer (Fig. 1) employing three X-Y multiwire proportional chambers (MWPC). The chambers (5000 wires altogether) have 2 mm spacing between signal wires and the left and right halves of the horizontal wires are divided to allow independent readout. The spectrometer magnet was operated at 210.6 MeV/c transverse momentum, between the maximum values possible for $\mu\mu$ and $\pi\pi$ decays. Electrons were detected in an atmosphere-pressure hydrogen-gas Cherenkov counter with twelve independent optical sectors. Following the spectrometer are three walls of heavy concrete, total thickness 900 g/cm^2, and three

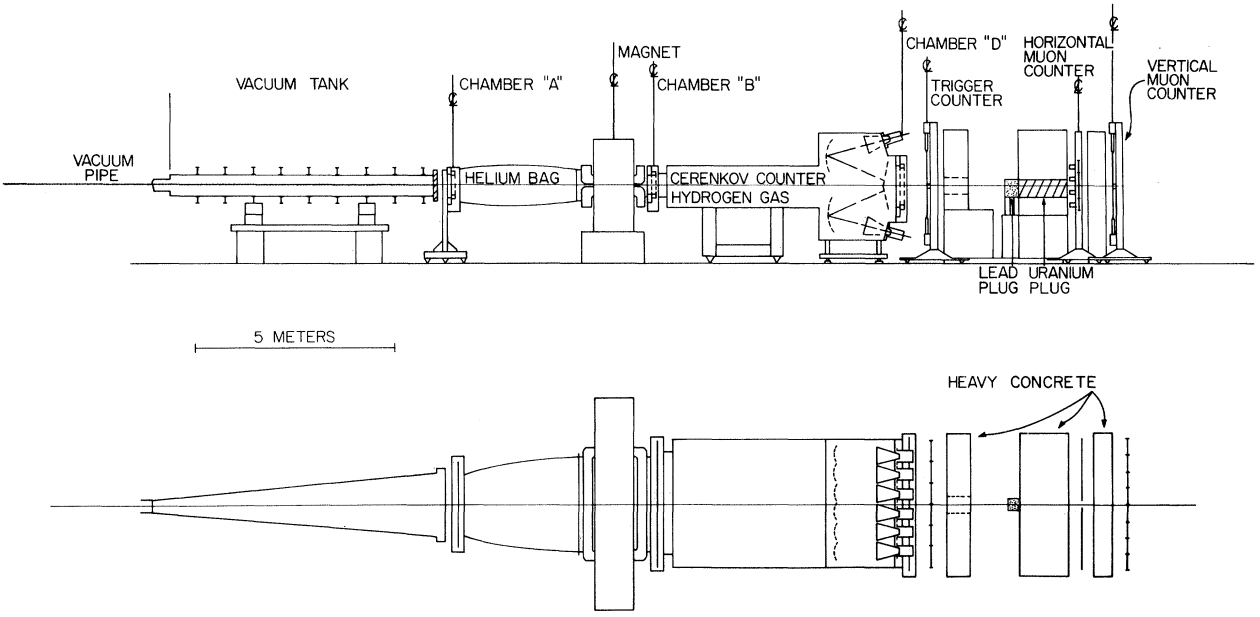

FIG. 1. Layout of the apparatus. MWPC's are chambers "*A*," "*B*," and "*D*."

planes of scintillation counters. The first plane of twelve counters precedes the absorber and is used primarily for the generation of an accurate timing signal for all K^0 decay modes. The second hodoscope consists of eight horizontal counters, four on each side of the beam, while the third array contains eight vertical counters. Pion and electron secondaries are strongly absorbed by the concrete, whereas muon secondaries above 1.8 GeV/c penetrate with high probability. The neutral beam is allowed to pass through a hole in the first wall and is absorbed by an insert of uranium and lead in the second wall.

Data were recorded when either of two trigger conditions were satisfied: (1) muon trigger—exactly two complete trajectories through the MWPC's, at least one hit in each of the three scintillation counter planes, and at least two hits in either the horizontal or vertical muon counters; (2) open trigger—exactly two complete trajectories through the MWPC's, and at least one hit in the first scintillation counter hodoscope. These events provided a monitor of the performance of the apparatus and a measure of the K_L^0 beam flux through the $\pi^+\pi^-$ decay mode. Only 1 in 64 of these tracks was actually recorded.

Both $\pi^+\pi^-$ and $\mu^+\mu^-$ candidates were required to meet the following criteria: (1) Decay vertex within a fiducial volume in the vacuum chamber. (2) Extrapolated secondary trajectories within the active area of the last (vertical) muon hodoscope. (3) Secondary momenta between 2 and 7 GeV/c, and K^0 momentum less than 12 GeV/c. The lower bound ensures efficient muon penetration of the concrete absorber and the upper bounds serve to reduce background from K_{μ_3} decays. (4) No signal in the Cherenkov counter.

For the $\pi^+\pi^-$ decay candidate, no muon counter may be hit. However, a muon is required to be detected in each of the two muon hodoscopes by counters that lie along the path of the particle; counter boundaries are enlarged slightly with a momentum-dependent correction to account for multiple scattering in the absorber. In addition, the trajectories for $\mu^+\mu^-$ decay candidates may not share any counters in either the horizontal or vertical hodoscope. To reduce possible contamination from pion or electron showers, any event with more than five muon counters hit is rejected. Independent studies of the muon detector using K_{μ_3} decays and stray muons from the alternating-gradient synchrotron demonstrate a detection efficiency of $>95\%$ for each muon.

The response of the spectrometer to $\mu^+\mu^-$ decays was studied in detail by means of several thousand of the kinematically similar $\pi^+\pi^-$ decays. An event was described by the vertical "kink" angle of each secondary, the closest distance of approach of the two trajectories in the decay region, the polar angle θ_K between the total vector momentum of the two secondaries and the incident K_L^0 direction, and finally the reconstructed invariant mass. Distributions of the

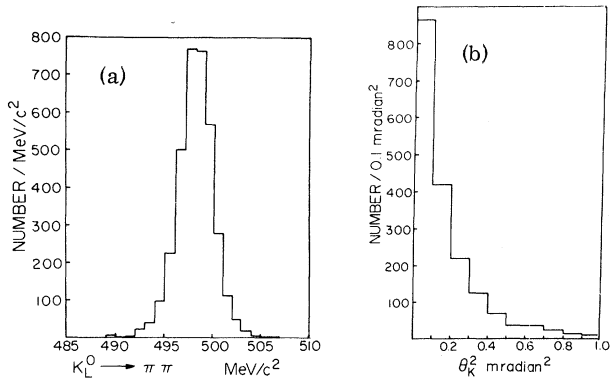

FIG. 2. (a) Invariant mass spectrum for the decay $K_L^0 \rightarrow \pi^+\pi^-$, subject to all cuts except in mass. (b) Spectrum of the variable θ_K^2, the polar angle between the reconstructed K_L^0 momentum and the direction defined by the decay vertex and production target.

first three "geometrical" variables yield widths consistent with the calculated resolution of the apparatus. Their χ^2 distribution is in excellent agreement with that expected for three degrees of freedom. All data with χ^2 greater than 6.25 have been rejected; this choice eliminates only 10% of the good events while strongly suppressing background from $\pi \rightarrow \mu\nu$ decays.

Distributions in θ_K and invariant mass of the $\pi^+\pi^-$ events are shown in Fig. 2. Averaged over the incident momentum spectrum ($\langle P_K \rangle = 7$ GeV/c), $\sigma_{\theta_K} = 0.52$ mrad and $\sigma_{m_{\pi\pi}} = 1.8$ MeV/c^2. The mean K_L^0 mass is measured to be 498.6 MeV/c^2, about 1 MeV/c^2 higher than the accepted value.

All $\mu^+\mu^-$ decay candidates surviving the χ^2 cut, with $\theta_K^2/\sigma_{\theta_K}^2 < 50$ and $M_{\mu\mu} > 480$ MeV/c^2, are shown in Fig. 3(b). The 2σ boundaries in both variables are indicated by the dashed lines. Six $\mu^+\mu^-$ events are found in the 2σ interval, $|M_{\mu\mu} - M_K| < 3.5$ MeV/c^2, and $\theta_K^2/\sigma_{\theta_K}^2 < 3$. For comparison, a similar distribution for about 100 $\pi^+\pi^-$ decay candidates is presented in Fig. 3(a).

Two projections of the $\mu^+\mu^-$ scatter plot are shown in Fig. 4: the mass spectrum for $\theta_K^2/\sigma_{\theta_K}^2 < 3$, and the angular distribution for events with $|M_{\mu\mu} - M_K| < 3.5$ MeV. No significant background at the K^0 mass in the forward direction is seen in either distribution. One estimate of the background may be easily made from the angular distribution: This background is expected to be independent of θ_K^2 since the range of the missing transverse momentum is much larger than the resolution. The three events in the interval $3 < \theta_K^2/\sigma_{K_2}^2 < 39$ yield an expected background of 0.25 ± 0.15 in the interval $\theta_K^2/\sigma_{\theta_K}^2 < 3$, $|M_{\mu\mu} - M_K| < 3.5$ MeV. The probability that the six observed

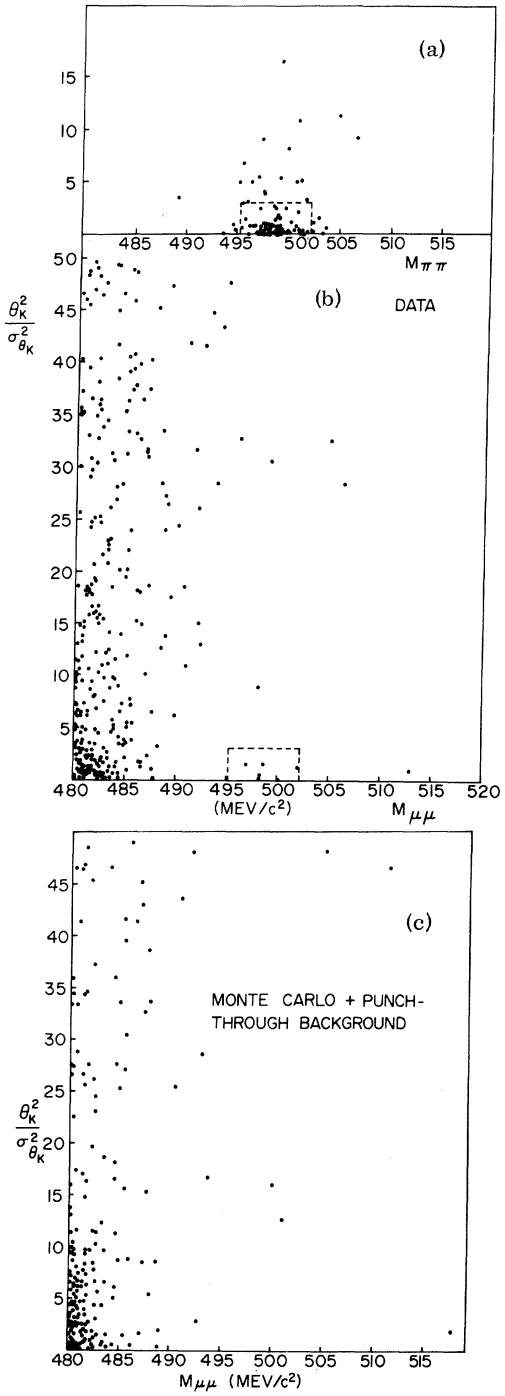

FIG. 3. (a) Scatter plot in the mass-angle plane for the decay $K_L^0 \rightarrow \pi^+\pi^-$, subject to the identical cuts used in the $\mu^+\mu^-$ analysis. The acceptance region is enclosed within the dashed lines. (b) Scatter plot in the mass-angle plane for all $K_L^0 \rightarrow \mu^+\mu^-$ decay candidates. (c) A simulation of the background in the $K_L^0 \rightarrow \mu^+\mu^-$ decay arising from the following two sources: (1) $K_L^0 \rightarrow \pi\mu\nu$ decays in which the π decays and completes the signature for two muons, and (2) $K_L^0 \rightarrow \pi\mu\nu$ decays in which the π punches through the μ filter and completes the signature for two muons.

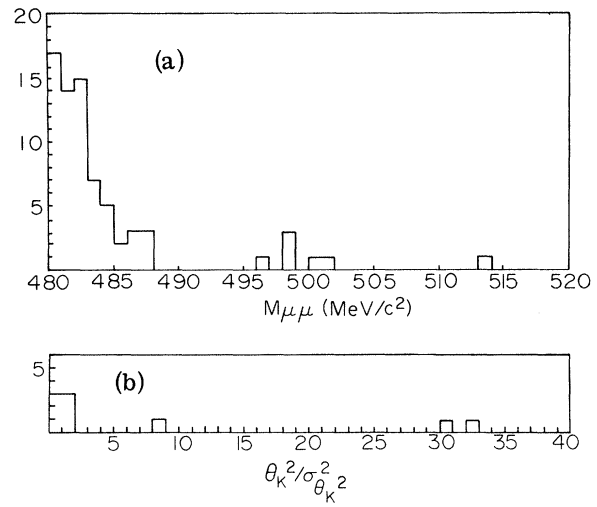

FIG. 4. (a) Projection of the $\mu^+\mu^-$ scatter plot on the mass axis for $\theta_K^2/\sigma_{\theta_K}^2 < 3$. There are no events at higher mass. (b) Projection of the $\mu^+\mu^-$ scatter plot on the angle axis for events with $|M_{\mu\mu} - M_K| < 3.5$ MeV.

events are a fluctuation of a smooth background is less than 0.1%. We conclude that these six events are indeed examples of the decay $K_L^0 \to \mu^+\mu^-$.

As for the remaining events in the scatter plot, only the processes $K_L^0 \to \pi\mu\nu$ with the pion penetrating the concrete absorber and $K_L^0 \to \pi\mu\nu$ with the pion decaying within the spectrometer have been found to contribute significantly.[4]

In the first case, if the pion is identified as a muon, but its momentum measured correctly, the apparent invariant mass cannot exceed 481 MeV/c^2. From a study of $\pi^+\pi^-$ decays, the probability of pion penetration has been measured to be $\approx 1.4\%$. Using this penetration factor, the contribution of this background process has been determined by reanalyzing $K_{\mu 3}$ decays (from the open trigger data) as if both particles were muons. These events are found to be the dominant contribution for $M_{\mu\mu} < 490$ MeV/c^2, $\theta_K^2/\sigma_{\theta_K}^2 < 10$.

In the second case when the pion decays, the corresponding deflection of the trajectory may contribute a substantial error in the momentum of the secondary, allowing invariant masses even greater than the K^0 mass. This source of background has been estimated by a Monte Carlo calculation. The combined contribution from both sources, shown in Fig. 3(c), is quite similar to the real data, although a discrepancy of about 30% exists in the total number of events.[5] In the region of the K^0 mass, nevertheless, there is no evidence for θ_K^2 peaking in the forward direction.

The $\pi^+\pi^-$ decays permit a direct determination of the branching ratio $\Gamma(K_L^0 \to \mu^+\mu^-)/\Gamma(K_L^0 \to \pi^+\pi^-)$. Correcting for the trigger suppression factor of 64, we find that our data correspond to 1.0×10^6 $\pi^+\pi^-$ decays. A Monte Carlo calculation of the relative acceptance $A_{\pi\pi}/A_{\mu\mu}$ was performed which included losses due to $\pi \to \mu\nu$ decays (18%), and also losses due to scattering out of muons in the absorber (7%). We find

$$\frac{\Gamma(K_L^0 \to \mu^+\mu^-)}{\Gamma(K_L^0 \to \pi^+\pi^-)} = \frac{N_{\mu\mu}}{N_{\pi\pi}}\frac{A_{\pi\pi}}{A_{\mu\mu}} = \frac{6}{1.0\times10^6}\times 1.12$$

$$= 6.7\times10^{-6}.$$

Finally,[6]

$$\frac{\Gamma(K_L^0 \to \mu^+\mu^-)}{\Gamma(K_L^0 \to \text{all})} = \frac{\Gamma(K_L^0 \to \mu^+\mu^+)}{\Gamma(K_L^0 \to \pi^+\pi^-)}\frac{\Gamma(K_L^0 \to \pi^+\pi^-)}{\Gamma(K_L^0 \to \text{all})}$$

$$= 6.7\times10^{-6}\times 1.57\times10^{-3}$$

$$= 11^{+10}_{-5}\times10^{-9}$$

(90% confidence level).

This value is clearly in good agreement with the unitarity bound, but in sharp disagreement with the result of Clark *et al.*[3] Based on the present experiment, the probability that the branching ratio is below 1.8×10^{-9} is less than 0.06%.

We wish to acknowledge numerous contributions of the staffs of Brookhaven National Laboratory and Nevis Laboratory to the success of the experiment.

---

†Research supported in part by the U.S. Atomic Energy Commission and the National Science Foundation.

*Sloan Foundation Fellow 1972–1974.

[1]L. M. Sehgal, Phys. Rev. 183, 1511 (1969); C. Quigg and J. D. Jackson, UCRL Report No. 18487 (unpublished).

[2]M. K. Gaillard, Phys. Lett. 35B, 431 (1971); A. D. Dolgov *et al.*, Yad. Fiz. 16, 149 (1972) [Sov. J. Nucl. Phys. (to be published)]; B. R. Martin *et al.*, Phys. Rev. D 2, 179 (1970); S. L. Adler *et al.*, Phys. Rev. D 5, 770 (1972).

[3]A. R. Clark *et al.*, Phys. Rev. Lett. 26, 1667 (1971).

[4]Other processes examined and found to contribute insignificantly are $K_L^0 \to \pi e\nu$, $K_L^0 \to \pi^+\pi^-$, $K_L^0 \to \pi^+\pi^-\pi^0$, $K_L^0 \to \mu^+\mu^-\gamma$, and two unrelated tracks in accidental coincidence.

[5]In this delicate calculation, substantial errors in the apparent normalization can arise from a number of sources. For example, a systematic momentum error $\Delta p/p$ of just 1.3% in the $\pi \to \mu\nu$ decay simulation would

cause the observed discrepancy. Uncertainties in the $K_{\mu 3}$ form factors also can contribute.

[6]Here we use the current world average for $\Gamma(K_L{}^0 \to \pi^+\pi^-)/\Gamma(K_L{}^0 \to \text{all})$ as obtained by the Particle Data Group, Lawrence Berkeley Laboratory Report No. 100, 1972 (unpublished).

Pion Condensation in Nuclear and Neutron Star Matter*

Gordon Baym
Department of Physics, University of Illinois, Urbana, Illinois 61801
(Received 13 April 1973)

The equilibrium thermodynamic conditions obeyed by a pion condensed system are given. These include the statement that the average spatial currents of conserved quantities must always vanish in the state of lowest free energy, even for π^- condensation into a running-wave mode. The physical significance of pion-condensation thresholds is also discussed.

The possibility that the pion field in dense nuclear or neutron-star matter may develop a macroscopically occupied mode, or condensate, has recently been explored by several authors.[1-4] In the normal state of these systems, the ground-state expectation values of φ_0, the neutral pion field, and φ, the charged (π^-) field, vanish as a result of parity conservation, and for $\langle\varphi\rangle$ as a result of charge conservation as well. Pion-condensed phases are states of broken symmetry, characterized by a nonvanishing $\langle\varphi\rangle$ for π^- condensation, while in a π^0 condensed system $\langle\varphi_0\rangle \neq 0$. The main purpose of this Letter is to derive the equilibrium thermodynamic conditions that are obeyed by the ground state, or, more generally at finite temperature, by the state of lowest free energy of a pion condensed system.

The first result we need, one familiar from the microscopic theory of superfluidity, is that the condensate wave function $\langle\varphi(\vec{r}, t)\rangle$ must vary in time as $\exp(-i\mu_\pi t)$, where μ_π is the π^- chemical potential. To see this we note that in a π^- condensed phase, the ground-state energy $E = \langle H\rangle$, or the free energy $F = E - TS$ at finite temperature, is a functional of $\langle\varphi(\vec{r}, t)\rangle$, $\langle\pi(\vec{r}, t)\rangle$ (where π is the momentum conjugate to φ), as well as $\langle\varphi^\dagger(\vec{r}, t)\rangle$ and $\langle\pi^\dagger(\vec{r}, t)\rangle$. For fixed expectation value of $\rho_\pi = i(\varphi^\dagger\pi - \pi^\dagger\varphi)$, the ground-state energy $\langle H\rangle$ must be a minimum under variation of $\langle\varphi\rangle$ and $\langle\pi\rangle$, or, under an arbitrary variation, $\delta\langle H\rangle = \mu_\pi\,\delta\langle\rho_\pi\rangle$. Consider a variation that adds c-number fields to $\langle\varphi\rangle$ and $\langle\pi\rangle$. Then since $\delta\langle\rho_\pi\rangle = i\langle\varphi^\dagger\rangle\,\delta\langle\pi\rangle + \delta\langle\varphi^\dagger\rangle \times\langle\pi\rangle + \text{c.c.}$, and $\delta\langle H\rangle = \langle\delta H/\delta\pi\rangle\,\delta\langle\pi\rangle + \langle\delta H/\delta\varphi\rangle\,\delta\langle\varphi\rangle + \text{c.c.}$, we have, on comparing coefficients of $\delta\langle\varphi^\dagger\rangle$, and of $\delta\langle\pi^\dagger\rangle$,

$$\langle\delta H/\delta\pi^\dagger\rangle \equiv \langle\dot{\varphi}\rangle = -i\mu_\pi\langle\varphi\rangle, \qquad \langle\delta H/\delta\varphi^\dagger\rangle \equiv -\langle\dot{\pi}\rangle = i\mu_\pi\langle\pi\rangle. \tag{1}$$

Thus

$$\langle\varphi(\vec{r}, t)\rangle = \exp(-i\mu_\pi t)\langle\varphi(\vec{r})\rangle, \qquad \langle\pi(\vec{r}, t)\rangle = \exp(-i\mu_\pi t)\langle\pi(\vec{r})\rangle. \tag{2}$$

The π^0 chemical potential vanishes and so for a condensed neutral π^0 field $\langle\varphi_0\rangle$ and $\langle\pi_0\rangle$ are constant in time.

The density of condensed π^-, the net charge associated with the macroscopically occupied pion mode, is given by $\langle\rho_\pi\rangle_{\text{cond}} = -2\,\text{Im}(\langle\varphi\rangle^*\langle\pi\rangle)$. When terms in the interaction Lagrangian containing $\dot{\varphi}$ can be neglected, as in the nonrelativistic limit of the pseudovector coupling, then $\pi = \dot{\varphi}$ and[5] $\langle\rho_\pi\rangle_{\text{cond}} = 2\mu_\pi|\langle\varphi(\vec{r})\rangle|^2$.

Combining Eqs. (1) we find the expectation value of the π^- field equation:

$$(\mu_\pi{}^2 - m_\pi{}^2 + \nabla^2)\langle\varphi(\vec{r})\rangle - J(\vec{r}) = 0, \tag{3}$$

where $J(\vec{r}) = -\langle\delta L_{\text{int}}/\delta\varphi^\dagger(\vec{r})\rangle - i\mu_\pi\langle\delta L_{\text{int}}/\delta\dot{\varphi}^\dagger(\vec{r})\rangle$ is the source of the condensed-pion field and L_{int} is the interaction Lagrangian. Equation (3) determines the condensate wave function in terms of the source $J(\vec{r})$. The threshold for π^- condensation is the first point at which the field equation (3) can be satisfied; below threshold $J(\vec{r}) = 0$. Expanding $J(\vec{r})$ to first order in $\langle\varphi(\vec{r}')\rangle$ and using $\delta J(\vec{r})/\delta\langle\varphi(\vec{r}')\rangle = \Pi(\vec{r}, \vec{r}'; \omega = \mu_\pi)$, the π^- self-energy in the medium, we see that the π^--condensation threshold is the point where $\int D^{-1}(\vec{r}, \vec{r}', \mu_\pi)\langle\varphi(\vec{r}')\rangle \times d^3r' = 0$, i.e., where the pion Green's function D, for $\langle\varphi\rangle = 0$, has a pole at frequency μ_π. Above the threshold, however, the amplitude of $\langle\varphi\rangle$ is determined by (3), not by the equation for D (which describes the fluctuations in the pion field). A point at which D_0, the π^0 Green's function (for $\langle\varphi_0\rangle = 0$), develops a pole at $\omega = \mu_{\pi 0} = 0$ would be a π^0 threshold.[1]